

The role of optineurin in the process of phagocytosis

Bulić, Katarina

Master's thesis / Diplomski rad

2022

Degree Grantor / Ustanova koja je dodijelila akademski / stručni stupanj: **University of Rijeka / Sveučilište u Rijeci**

Permanent link / Trajna poveznica: <https://um.nsk.hr/um:nbn:hr:193:962680>

Rights / Prava: [In copyright](#)/[Zaštićeno autorskim pravom.](#)

Download date / Datum preuzimanja: **2024-11-16**

Repository / Repozitorij:



[Repository of the University of Rijeka, Faculty of Biotechnology and Drug Development - BIOTECHRI Repository](#)



UNIVERSITY OF RIJEKA
DEPARTMENT OF BIOTECHNOLOGY
Graduate program
Drug research and development

Katarina Bulić

The role of optineurin in the process of phagocytosis

Master's thesis

Rijeka, 2022

UNIVERSITY OF RIJEKA
DEPARTMENT OF BIOTECHNOLOGY
Graduate program
Drug research and development

Katarina Bulić

The role of optineurin in the process of phagocytosis

Master's thesis

Rijeka, 2022

Mentor: Ivana Munitić, MD, PhD

Master's thesis was defended on September 27th, 2022

in front of the committee:

1. Željka Minić, PhD
2. Dragomir Milovanović, PhD
3. Ivana Munitić, MD, PhD

The thesis has 45 pages, 10 figures, 0 tables, and 43 references

Abstract

Optineurin is an adaptor protein implicated in multiple cellular processes, such as autophagy, vesicular trafficking, exocytosis, and inflammation. Mutations in the optineurin gene have been linked with amyotrophic lateral sclerosis (ALS), a neurodegenerative disease impacting motor neurons. Previous research has found that phagocytosis, the process of removing extracellular particles by professional phagocytic cells, was disrupted in ALS, and research from our laboratory on cell lines has shown slightly impaired phagocytosis in optineurin deficient cells. The goal of this thesis was to research the role of optineurin in phagocytosis using primary cells. To do that, we performed a flow cytometry-based assay on primary wild type (WT) and optineurin-insufficient OPTN^{470T} bone marrow-derived macrophages (BMDMs) generated from mice aged 3 months and 2 years and microglia generated from neonatal mice. We found no difference between the genotypes in the number of phagocytic cells or their phagocytic ability in basal condition in neither BMDM nor microglia. The same lack of difference persisted when primary cells were pre-treated with inflammatory stimuli, as well as when degradation through autophagy and lysosomes was blocked. Interestingly, we found that phagocytosis was impaired in BMDMs from older mice compared to BMDMs from younger mice, but the difference was not significant when cells were pre-treated with an inflammatory stimulus. In conclusion, this study did not confirm the role of optineurin in phagocytosis of neuronal debris by primary cells, but the difference in the level of phagocytosis between cells generated from younger and older mice opens up a new route of research.

Key words: optineurin, amyotrophic lateral sclerosis, neurodegeneration, inflammation, phagocytosis

Sažetak

Optineurin je adaptorski protein uključen u više staničnih procesa kao što su autofagija, promet vezikula, egzocitoza i upala. Mutacije optineurina nedavno su se povezale s amiotrofičnom lateralnom sklerozom (ALS-om), neurodegenerativnom bolešću koja pogađa motoričke neurone. Prijašnja istraživanja pokazala su da je fagocitoza, proces u kojem profesionalni fagociti uklanjaju izvanstanične čestice, ometena u ALS-u. Istraživanja iz našeg laboratorija na staničnim linijama pokazala su da stanice bez optineurina imaju nešto nižu razinu fagocitoze. Cilj ovog istraživanja bio je vidjeti u primarnim stanicama ima li optineurin ulogu u procesu fagocitoze. U tu svrhu proveli smo esej fagocitoze baziran na protočnoj citometriji. Za istraživanje smo koristili wild type (WT) i OPTN^{470T} optineurin insuficijentnu mikrogliju dobivenu iz neonatalnih miševa, kao i makrofage dobivene iz koštane srži miševa starih 3 mjeseca i 2 godine. Nismo našli razliku između ova dva genotipa u broju stanica koje fagocitiraju niti u njihovoj sposobnosti fagocitoze u bazalnom stanju. Razlike nije bilo niti nakon tretmana stanica s upalnim stimulansima, kao ni kad se blokirala razgradnja autofagijom i lizosomima. Zanimljiva je bila razlika između BMDM-ova iz mladih i starih miševa koja je prestala biti značajna nakon što su stanice bile tretirane upalnim stimulusom. Zaključno, ovo istraživanje na primarnim stanicama nije potvrdilo ulogu optineurina u procesu fagocitoze neuronalnog otpada. Razlika u razini fagocitoze između primarnih stanica dobivenih iz mladih i starih miševa otvara nove mogućnosti u istraživanju ovog staničnog procesa.

Ključne riječi: optineurin, amiotrofična lateralna skleroza, neurodegeneracija, upala, fagocitoza

Contents

Abstract	4
Sažetak.....	5
1. Introduction	8
1.1 Amyotrophic lateral sclerosis	8
1.2. Optineurin	9
1.2.1. Models for optineurin research	11
1.3. Immune system in ALS.....	12
1.3.1. Neuroinflammation	13
1.3.2. Neuroinflammation and aging.....	15
1.4. Phagocytosis	15
1.4.1. Detection of the target particle	16
1.4.2. Activation of the internalization process.....	17
1.4.3. Phagosome formation.....	18
1.4.4. Phagosome maturation.....	18
1.4.5. Phagocytosis in ALS	19
2. Thesis goals	20
3. Materials and methods.....	22
3.1. Isolation of primary microglia and macrophages.....	22
3.2. Primary cell counting and staining.....	23
3.3. Cell treatments.....	24
3.4. Phagocytosis assay	24
3.5. Flow cytometry	27
3.6. Statistical analysis	29
4. Results	30
4.1. Frozen N2A debris does not affect phagocytosis in WT and OPTN ^{470T} BMDMs.....	30

4.2. Optineurin insufficiency does not diminish phagocytosis of N2A debris in BMDMs from young mice.....	32
4.3. Optineurin insufficiency does not diminish phagocytosis of N2A debris in BMDMs from aged mice	33
4.4. Phagocytosis in WT and OPTN ^{470T} BMDMs becomes impaired with age	35
4.5. Optineurin insufficiency does not diminish phagocytosis of dN2A in WT and OPTN ^{470T} microglia	36
5. Discussion.....	38
6. Conclusion	41
7. Literature.....	42

1. Introduction

1.1 Amyotrophic lateral sclerosis

Amyotrophic lateral sclerosis (ALS), also known as Lou Gehrig's disease, is a fast progressing neurodegenerative disease causing loss of both upper and lower motor neurons in the central nervous system (CNS) (1). Upper motor neurons are situated in the motor cortex in the frontal lobe, whereas lower motor neurons are situated in the brainstem, and in the ventral horn part of the spinal cord (1). Overwhelming majority of patients die within a few years of the symptom onset (median survival period is around 3 years), with only 10% of patients surviving longer (up to 10 years) (1). Symptoms vary, but common hallmarks of ALS are muscle weakness and paralysis, and the disease becomes fatal once respiratory muscles are affected (1,2).

ALS is a rare disease, with an incidence of 1.75 in 100,000 people (3). It is slightly more frequent in men than in women (ratio of 1.68). Average age of onset is middle to late 50s. An earlier onset in late teenage to early adult years is more common in patients with family history of the disease (1,4). The latter comprise 10% of all ALS cases (familial ALS or fALS), whereas 90% are sporadic (sALS). Both fALS and sALS have had genetic mutations associated with them (4). The first ALS-linked mutation was found in the gene superoxide dismutase-1 (SOD1) in 1993, and since then studies have found more than 30 genes connected to ALS (1). Chromosome 9 open reading frame 72 (*C9orf72*) is one such gene, with mutations found in 40% of fALS cases in Caucasians, making it the most frequent ALS mutation. Genes encoding SOD1, TAR-DNA-binding protein of 43 kDa (TDP-43), TANK-binding kinase-1 (TBK1), fused in sarcoma (FUS), and optineurin (OPTN) proteins are other notable mutations, but are present in a small subset of patients (1,5,6). Notably, mutation frequency differs in different populations, but it is not possible to determine whether it is due to a genetic factor, or an environmental one (3).

Even with many identified genetic factors, the fundamental mechanisms of ALS pathology are not fully understood, and several mechanisms have been proposed, including impaired proteostasis, oxidative stress, excitotoxicity, mitochondrial dysfunction, disrupted vesicular transport, and others (1). As with other neurodegenerative disorders, such as Parkinson's or Alzheimer's disease, one of the key hallmarks of ALS are protein aggregates. A large percentage of ALS patients have aggregates of TDP-43 protein (97%) (7). In healthy conditions TDP-43 is mostly localized within the cell nucleus, where it acts a regulator of RNA transcription, alternative splicing, and other steps of RNA metabolism (8,9). Mutations in the gene encoding TDP-43 are a rare cause of the disease, though (less than 5%), and it's the wild-type protein that's predominantly found in the cytoplasmic aggregates (1,8). Hence, it is not clear whether the disease develops because of a loss-of-function of TDP-43 due to mislocalization to the cytoplasm, because of a toxic gain-of-function due to aggregation, or both (8,10).

One protein that was recently implied in ALS is optineurin, an adaptor protein involved in many cellular progresses, such as vesicle trafficking, autophagy, Golgi processes, and inflammation regulation (10). *OPTN* mutations implicated in ALS are thought to be loss-of-function (1,7,10,11). Proteins interacting with *OPTN*, such as TANK-binding kinase 1 (TBK1) and p62, have since been found to have a disrupted function in ALS. TBK1 and p62 are also involved in both inflammation and autophagy, suggesting that there is an interconnected mechanism network disrupted in ALS (11,12).

1.2. Optineurin

Optineurin is a cytoplasmic protein. In humans, it is encoded by the *OPTN* gene on the tenth chromosome and made up of 577 amino acids. Its name comes from 'optic neuropathy inducing' given that *OPTN* mutations were found in patients suffering from primary open-angle glaucoma (13).

Optineurin is a ubiquitin binding protein, containing a ubiquitin-binding region on its C-terminus. Ubiquitination is posttranslational modification where

proteins are marked for degradation through the ubiquitin proteasome system (UPS) or trafficking through the cell. Ubiquitin ligases are enzymes that conjugate the C-terminus of ubiquitin to lysines (K) of target proteins. This modification often includes polyubiquitin chains, formed through ubiquitin self-conjugation on any of its lysines (K6, K11, K27, K29, K33, K48, AND K63) or the methionine on the N-terminus (M1). Optineurin shows a preference for M1 and K63-linked polyubiquitin chains. Those chains facilitate recruitment of adaptor or regulatory proteins for cell signaling mediation (10).

The exact physiological function of optineurin is still unclear, but it has been proposed that it functions as a regulatory and adaptor protein in several cellular processes. Some of the optineurin-interacting proteins are myosin VI, huntingtin (htt), rab8, and microtubule-associated 1A/1B-light chain-3 (LC3). All these proteins are involved in autophagy, exocytosis, and vesicular trafficking (7). Optineurin has been proposed to act as a regulator in nuclear factor kappa-light-chain-enhancer of activated B cells (NF- κ B) signaling pathway, which has a role in innate immunity and inflammation (10). Optineurin also interacts with TBK1, a kinase necessary for the production of type I interferons (IFN) (10,12).

Around 40 OPTN mutations have been found in ALS patients. The majority are point mutations, both missense and nonsense mutations, while the rest includes frameshift mutations, deletions, and null mutations (10). The effects of most of the mutations are still not known, and very few of them have been confirmed to be pathogenic. Some of the *OPTN* mutations that are implicated in ALS are E478G point mutation and Q398X and Q165X nonsense mutations, all of which affect the ubiquitin binding region of optineurin on its C-terminus (2,11).

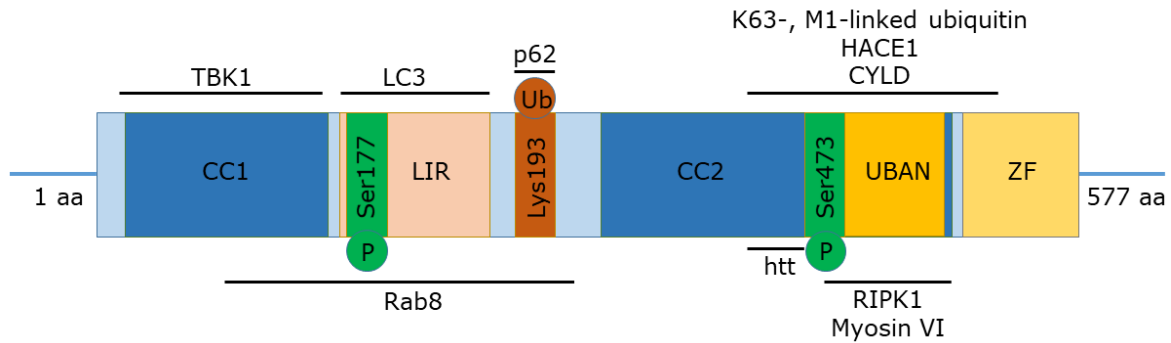


Figure 1 Schematic representation of optineurin domains and its interacting partners. The coiled-coil 1 (CC1) domain on the N-terminus interacts with TBK1. Next follows the LC3-interacting region (LIR), and the Ser177 amino acid, which is phosphorylated by TBK to enhance the binding between LC3 and optineurin. HACE1 ubiquitin ligase ubiquitinates optineurin on Lys193, a modification necessary for binding of p62 to optineurin. The coiled-coil 2 (CC2) domain is important for the self-oligomerization of optineurin, a process important for binding linear ubiquitin. Ubiquitin-binding domain (UBAN) on the C-terminus is important for binding polyubiquitinated cargo, such as bacteria, protein aggregates, or damaged mitochondria. This domain is important for binding RIPK1, a regulator of an inflammatory pathway, as well as myosin VI, a protein important for autophagy and vesicle trafficking. Modified from Prtenjaca et al., 2020.

1.2.1. Models for optineurin research

Both *in vitro* and *in vivo* models have been used to study the effect of optineurin deficiency. Some murine models focused on ubiquitin-binding activity of optineurin. Model Optn^{D477N} carries the D477N point mutation which imitates the human E478G mutation in mice, and it fails to bind ubiquitin (14). Model Optn^{470T} has a STOP codon after amino acid 470, and the truncated optineurin with this mutation lacks the entire ubiquitin binding domain. The optineurin in this model is not only truncated, but present in lesser amounts, making it a model of optineurin insufficiency (15). Other models focused on a different part of the protein. Model Optn Δ^{157} is lacking the first 157 amino acids on the N-terminus, completely inhibiting the protein's TBK1-binding activity (16). A model completely lacking optineurin (Optn^{-/-}) has also been established (17). Cell lines may not perfectly represent live organisms and their cells, but *in vitro* research featuring cell lines is still valuable. With advantages such as easier manipulation than animal models or primary cells,

and the fact they can be passaged, cell line research can give good first insights into possible mechanisms of action of certain cellular processes. Different cell lines that are often used in optineurin research are human cervical cancer cells (HeLa), murine neuroblastoma cells (Neuro2A, N2A), and human embryonic kidney cells (HEK293) (18–20).

1.3. Immune system in ALS

Neurons are not the only cells present in the CNS; a number of other cells, called the glial cells keep, the CNS in order and maintain homeostasis. These glial cells include microglia, astrocytes, oligodendrocytes, and ependymal cells. Astrocytes provide trophic and structural support to neurons, supplying growth factors and nutrients while also maintaining the blood-brain barrier (BBB). Microglia are the only resident immune cells in the CNS. Their task is surveying the CNS, and once they are activated, triggering an inflammatory response against different neurotropic infectious agents, as well as clearing out debris through the process of phagocytosis (21).

There is abundant evidence supporting the theory that non-neuronal cells play a large role in ALS. Selective expression of human superoxide dismutase 1 (hSOD1) mutation in neurons wasn't enough to cause neuronal death, implying that non-neuronal cells carrying that mutation contribute to the pathology (22). Likewise, healthy glia surrounding diseased neurons in chimeric mice with hSOD1 mutation were able to alleviate the disease (23). Deletion of hSOD1 mutant in motor neurons delays the onset of the disease, but it does not protect from disease progression and death, showing that glial cells with the hSOD1 mutation are sufficient to trigger neuronal death. In contrast, selective deletion of the hSOD1 mutation in myeloid cells (microglia and macrophages) or in astrocytes does not affect the disease onset, but slows the progression and increases life span (24,25). Taken together, these findings indicate that mechanisms of ALS affect not only motor neurons, but also glial cells.

1.3.1. Neuroinflammation

Neuroinflammation is inflammation in the CNS, and is primarily orchestrated by microglia upon activation by different DAMPs and PAMPs, such as LPS and heat shock proteins. Different proteins that aggregate in ALS, such as TDP-43 and SOD1, also bind to these receptors (21,26).

Microglial response to acute and chronic injury differs. Once activated, their morphology changes (enlarged cell body and thickened processes), they start proliferating, producing reactive oxygen and nitrogen species (ROS, RNS) and pro-inflammatory cytokines like TNF- α and IL-1 β . They also increase their phagocytic potential (21). This kind of activation has been described as the M1 or classical phenotype (Figure 3), although the terms are mostly avoided nowadays since polarization *in vivo* in neurodegenerative diseases is not as clear-cut as in the *in vitro* polarization experiments (21,27). The pro-inflammatory response leads to clearing out cellular debris, but it also triggers an anti-inflammatory response, which promotes neuronal repair and suppresses inflammation. These microglia, called M2 or alternatively activated microglia (Figure 3) release anti-inflammatory and neurotrophic factors such as interleukins 4 and 10 (IL-4, IL-10), brain-derived neurotrophic factor (BDNF), and arginase 1 (35). Unlike acute inflammation, in chronic inflammation there is constant release of the pro-inflammatory factors, and microglia do not follow the transition from the M1 to the M2 phenotype. It is difficult to detect the initial acute phase in ALS, suggesting that the damage done to CNS at first is subtle or that the switch from pro- to anti-inflammatory response happens smoothly (21). Studies done on hSOD1 mice models of ALS have shown that presymptomatic microglia release anti-inflammatory factors such as IL-10, and increasing IL-10 production in microglia delays the onset of the disease and increases survival, suggesting a potential neuroprotective role for these cells (36). During a prolonged exposure to damage and symptom onset, microglia increase the production of pro-inflammatory

factors, such as IL-1 β , IL-6, TNF- α , which in the end leads to neuronal damage once the pro-inflammatory environment becomes too much to contain through negative co-stimulation (30,31).

Of note is that microglia in the most affected lumbar region of the spinal cord in ALS are less responsive to stimuli than healthy microglia (21). This phenotype that is seemingly showing exhaustion and desensitization has been found in other neurodegenerative disorders, such as Alzheimer's disease and in mouse model of multiple sclerosis, experimental autoimmune encephalomyelitis, and has been named disease-associated microglia (DAM). This phenotype shows higher phagocytic and pro-inflammatory activity, but its role in ALS is not yet clear (21).

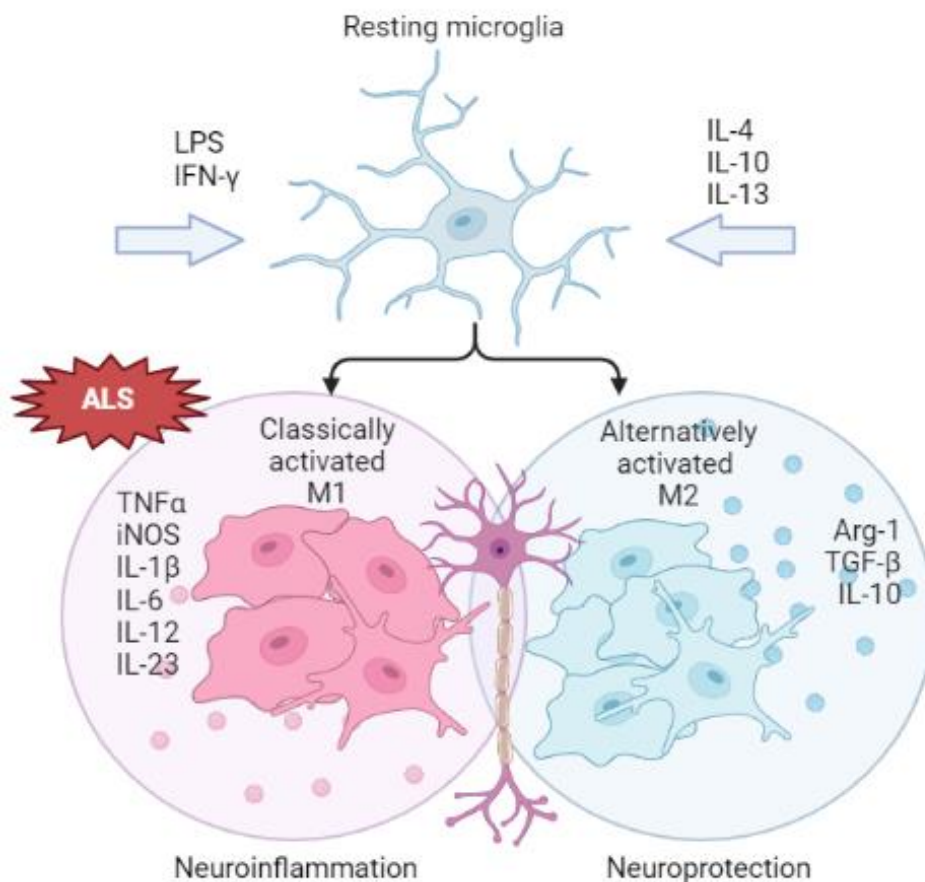


Figure 2 Role of microglia in ALS. In steady state microglia have small cell body and long processes. When activated through an external stimulus like IL-4 or LPS, microglia become amoeboid in shape, with large cell body and short processes. When activated by LPS or IFN- γ , resting microglia are induced into a classically activated or M1 phenotype which secretes pro-inflammatory cytokines (IL-1 β , IL-6, IL-12, IL-23, TNF- α , iNOS), causing inflammation and clearing out debris through their heightened phagocytic potential. When activated by anti-inflammatory factors, such as IL-4 and IL-10, the alternatively activated or M2 phenotype is induced, and is characterized by suppression of inflammatory response and promoting secretion of neurotrophic factors. Balance between these two phenotypes is crucial for proper clearance of damage and subsequent regeneration of tissue. In final stages of ALS, the chronic inflammation disturbs this balance, and the neuroinflammatory phenotype is overpowering, causing lasting neuronal damage. Modified from Béland et al., 2020 (27) and created with BioRender software.

1.3.2. Neuroinflammation and aging

Aging is a multifactorial process resulting from the interaction of lifestyle, environmental, and genetic variables. The risk of all neurodegenerative disorders increases with age. One of the possible reasons because aged organisms exhibit increased propensity for inflammation. This low level of chronic neuroinflammation and an increase in inflammatory response that accompanies aging of neurons is referred to as 'neuroinflammaging' (32).

The process of neuroinflammaging may lead to an increase in oxidative stress and the release of ROS, activating and influencing inflammatory pathways such as NF- κ B and causing apoptosis. TLRs have been shown to be expressed more in the aged brain, possibly causing increased activation of pro-inflammatory pathways and microglial activation (33). Microglia themselves have been shown to degenerate and become less functional with age (34), indicating that perhaps lack of debris clearance may be one of the causes of neuronal death.

1.4. Phagocytosis

Phagocytosis is the biological process of engulfing extracellular particles with a diameter larger than 0,5 μ m, such as cell debris or bacteria into phagocytic cells, which then degrade them. Professional phagocytic cells, those that are highly efficient in accomplishing phagocytosis include dendritic cells, neutrophils, macrophages and microglia. The particles are engulfed into an

organelle called phagosome, which then changes its membrane structure and content composition in the process of phagosome maturation. It next fuses with a lysosome and becomes a phagolysosome, an organelle that contains lytic enzymes that capable of degrading the ingested particles. There are several stages to phagocytosis: the detection of the target particle that is going to be ingested, the activation of the internalization process, the formation of the phagosome, and the phagosome maturation (Figure 4) (35).

1.4.1. Detection of the target particle

The detection of the target particle is the first step in phagocytosis. The detection is mediated by receptors on phagocytic cells. There are two kinds of receptors: non-opsonic, which directly bind PAMPs and are able to induce phagocytosis, and opsonic, which label the particles for and promote phagocytosis in that way (35).

Damaged or stressed cells release "find-me" signals to attract macrophages to their position (36). An example of these "find-me" signals are nucleotides, such as uridine triphosphate (UTP), adenosine triphosphate (ATP), and adenosine diphosphate (ADP). Chemokine (C-X3-C motif) ligand 1 (CX3CL1), also known as fractalkine is a strong "find-me" signal. Synapses and neurons release fractalkine to activate microglial CX3CR1 receptor.

Cells undergoing apoptosis are eliminated through phagocytosis, and they release "eat-me" signals, which are recognized by phagocytic cells (36). These "eat-me" signals include phosphatidylserine (PS) and lysophosphatidylcholine, and they appear on the surface membrane of apoptotic cells. Receptors recognizing PS directly are T cell immunoglobulin mucin (TIM) -1 and -4, stabilin-2, and brain-specific angiogenesis inhibitor 1 (BAI-1) (35). Some cells which are not undergoing apoptosis, such as activated T and B lymphocytes, also express large quantities of PS on their surfaces. These cells also express so called "do-not-eat-me" signals, such as the molecule CD47, a ligand to the signal regulatory protein α (SIR α) receptor, and which triggers a signaling

cascade which inhibits the signal for actin assembly, a crucial step in formation of the phagosome (35).

Oponic receptors bind opsonins, specific host-derived molecules which bind to the target particle and make it more susceptible to phagocytosis. Two groups of best studied opsonins that promote phagocytosis are antibodies and complement proteins. Fcγ receptors (FcγR) are glycoproteins which bind the Fc part immunoglobulin G (IgG) molecules. When they bind the antibody molecule, they are clustered on the cell membrane and trigger phagocytosis and other cellular processes. There are three types of FcγR expressed on human cells: FcγRI (CD64), FcγRII (CD32), and FcγRIII (CD16) (35).

Complement receptors (CRs) are receptors which bind activated complement components on microorganisms or cells. They are sorted into three groups: CR1 and 2 are formed by short consensus repeat elements, CR3 and 4 belong to the β2 integrin receptor family, and CR1g belongs to the Ig family (35).

1.4.2. Activation of the internalization process

Once the target particle is recognized by the receptors, phagocytosis is induced through various signaling pathways. The actin cytoskeleton rearranges and the membrane changes to form a depression in the area touching the particle, known as the phagocytic cup. Pseudopods then form and fuse until the particle is completely covered and inside a newly formed phagosome. Signaling pathways are best investigated for Fc receptors and complement receptors, and they differ in a few ways. While Fc-mediated phagocytosis includes forming of pseudopods around the target particle, CR-mediated phagocytosis includes “sinking” of the target particle into the membrane. Cytoskeleton usage for particle internalization also differs; Fc-mediated phagocytosis uses actin cytoskeleton, while CR-mediated phagocytosis uses actin and microtubule cytoskeletons (35).

1.4.3. Phagosome formation

The membrane changes its composition while the phagosome forms. Different lipids form and degrade on the phagosome membrane. Actin cytoskeleton also changes in order to form the pseudopodia that will engulf the target particle. After the cytoskeleton is disrupted, pseudopodia form through F-actin polymerization. Actin is depolymerized at the base of the phagocytic cup and the membrane of the phagosome is sealed at the distant end (35).

1.4.4. Phagosome maturation

The newly formed phagosome merges with early endosomes in a membrane fusion process regulated by the enzyme Rab5. Rab5 recruits molecules which promote the fusion of the newly formed phagosome with early endosomes. Despite the phagosome combining with several of these endosomes, it does not increase in size because recycling endosomes are being removed from the phagosome at the same time. Rab5 is lost in the process of phagosome maturation, and is replaced by Rab7 on the membrane, and this enzyme mediates the fusion of late endosomes with the phagosome. Vacuolar-type ATPase (V-ATPase) accumulates on the membrane phagosome at the same time, and is responsible for the acidification of the phagosome interior (pH 5.5 – 6.0) by moving protons (H^+) into the phagosome lumen. At the last stage, phagosomes merge with lysosomes to form phagolysosomes. This new organelle is equipped with mechanisms for microorganism degradation (low pH, production of ROS molecules, and hydrolytic enzymes) (35).

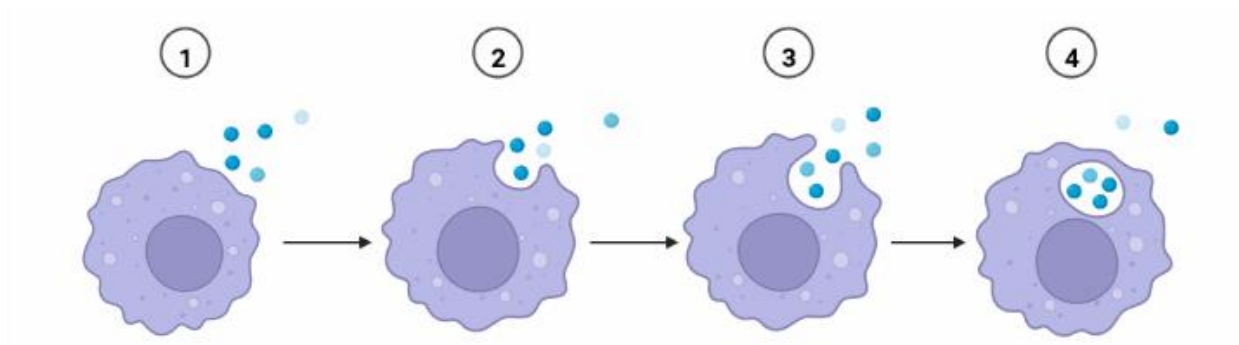


Figure 3 Process of phagocytosis. Once phagocytic cells recognize the “find-me” signals, they approach the target particles (1). Receptors directly recognizing “eat-me” signals or opsonins trigger a signaling cascade that leads to changes to the membrane as phagosome begins to form (2). Once the target particle is engulfed by pseudopodia (3), an early phagosome is formed (4) and begins the process of maturation. Figure created in BioRender software.

1.4.5. Phagocytosis in ALS

Multiple studies showed that phagocytosis might play a role in ALS progression. Activated phagocytic microglia were found in lumbar spinal cords of presymptomatic hSOD1 transgenic rats before any neuronal cell loss was detected (37). Furthermore, microglia-like cells derived from monocytes of sALS patients showed impaired phagocytosis. The impairment followed a trend that matched the disease progression (38). A study done in our lab on WT and OPTN knock-out (KO) BV2 microglial cell lines showed a mildly impaired phagocytosis in the OPTN KO cells (39).

2. Thesis goals

Optineurin has been proposed to participate in a wide array of cellular functions, including autophagy, inflammation, vesicular trafficking and others (10,11), and mutations in the OPTN gene were found in ALS patients (11), but the role in its pathology is yet unclear.

Phagocytosis is a crucial process in maintaining homeostasis by clearing out debris, and studies have shown it to be impaired in animal ALS models and primary cells derived from sALS patients (37,38). A flow cytometry-based assay was set up in our lab on WT and KO BV2 microglial cell lines (39), and here we have decided to repeat that experiment on WT and OPTN^{470T} primary cells (BMDMs and microglia).

Considering that the risk of neurodegenerative disorders increases with age, and that microglia degenerate and become less efficient as we get older (34), we have decided to perform the phagocytosis assay on BMDMs derived from mice aged 2 years.

Therefore, this thesis had the following goals:

1. Modifying experimental setup by comparing phagocytosis of fresh and frozen material (N2A and primary cortical neurons) using a flow cytometry-based assay as previously established in our laboratory (39)
2. Comparing phagocytosis efficiency of primary WT and OPTN^{470T} BMDMs generated from young mice using the improved phagocytosis assay set up in goal number 1
3. Comparing phagocytosis efficiency of primary WT and OPTN^{470T} BMDMs generated from old mice to see the effect of age-related immune dysfunction

4. Comparing phagocytosis efficiency of primary WT and OPTN^{470T} microglia derived from neonatal mice
5. Testing whether the inflammatory stimuli (LPS, poly(I:C)) would increase phagocytosis and/or uncover the differences between WT and OPTN^{470T} primary BMDMs and microglia
6. Testing whether blocking autophagy and/or lysosomal degradation would lead to signal accumulation

3. Materials and methods

3.1. Isolation of primary microglia and macrophages

The experiments were done on primary mouse BMDMs and microglia. Microglia was isolated by other laboratory members as described in (40). Cortical neurons for testing optimal experimental setup was received from other laboratory members and generated as described in (41). Wild type (WT) genotype was compared to OPTN^{470T/470T} genotype, which lacks the ubiquitin binding region (referred to as OPTN^{470T} cells). BMDMs were cultivated from bone marrow of mice. Mice aged 2 years and 3 months were sacrificed via cervical dislocation. The mice were placed on their back and sprayed with 70% ethanol. After separating the muscles from the skin, their hind legs were cut off below the hip and the feet were removed. The bones were cleaned of flesh in a Petri dish to gain access to the bone marrow and then moved to a new Petri dish containing complete RPMI. The bone marrow was flushed using a 3 mL syringe with a 25G needle. The medium containing bone marrow was filtered through a 40 µm cell strainer into a 50 mL Falcon tube and centrifuged (5 minutes, 1500 rpm). Supernatant was thrown away after the centrifuge, and bone marrow pellets was resuspended in the complete BMDM medium. Cells were then either moved to a Petri dish in complete BMDM medium and grown in an incubator (37°C, 5% CO₂) for 5 days, or until the cells were confluent. N2A cells were used as debris for phagocytosis experiments. N2A cells were grown in Petri dishes in Eagle's Minimum Essential Medium (EMEM, Capricorn) supplemented with 10% fetal bovine serum (FBS, Pan-Biotech), 1% 4-(2-hydroxyethyl)-1-piperazineethanesulfonic acid (HEPES, Capricorn), 1% Penicillin/Streptomycin/Amphotericin B Mix (Capricorn), 1% L-glutamine (Capricorn), referred to as complete EMEM (Capricorn). BMDMs were cultured Petri dishes in Roswell Park Memorial Institute (RPMI) medium (Capricorn), with all the supplements as complete EMEM, and with addition of 30% of L929 supernatant, referred to as complete BMDM medium. L929 is a mouse

fibroblast cell line that secretes macrophage colony-stimulating factor (M-CSF) in the supernatant, a growth factor necessary for macrophage differentiation from precursors found in bone marrow. Microglia were cultured in Dulbecco's Modified Eagle Medium (DMEM, Capricorn) with all the supplements as complete EMEM. Cells were maintained in an incubator at 37°C and 5% CO₂.

3.2. Primary cell counting and staining

Once confluency was reached, the cells were washed with Dulbecco's phosphate-buffered saline (PBS, Capricorn) and incubated with 10 mM EDTA (Carl Roth) for 15 min at 37°C. The dish was then rinsed with EDTA and complete RPMI to lift the cells. The cell suspension was then moved to a 50 mL Falcon tube and centrifuged (5 min, 1500 rpm). Supernatant was removed and the pellet was resuspended in 1-5 mL of complete BMDM medium. Live cells were counted using a Neubauer chamber, 10 µL of cell suspension was mixed with 90 µL of trypan blue. Number of live cells was calculated using the formula:

$$N(\text{cells/mL}) = \frac{N(\text{live cells}) \times \text{dilution in trypan blue} \times 10^4/\text{mL}}{N(\text{squares})}$$

(Note: 10⁴/mL refers to the volume of one large square in the Neubauer chamber, 1 mm x 1 mm x 0,1 mm = 10⁻⁴ mL = 10⁴/mL)

Once counted, BMDMs were stained with PKH26 (Sigma Aldrich) for future flow cytometry analysis, a red-fluorescent lipophilic cell membrane dye. 3 x 10⁶ cells were moved to a 15 mL Falcon tube and washed two times with RPMI medium without supplements (5 min, 1500 rpm). After the final washing, cells were resuspended in 100 µL of PBS. PKH26 was added (1:100 dilution in PBS) and the cells were incubated for 3 minutes in the dark at room temperature. PKH26 was neutralized with 200 µL of complete RPMI and washed three times

with 1 mL of complete RPMI (5 min, 1500 rpm). Cells were then counted again and plated on a 24-well plate at a density of 100 000 cells/well.

The same procedure was done on primary microglia, but since the laboratory had run out of the PKH26 dye, CellTrace FarRed (Invitrogen), a dye that covalently binds to free amines on the cell surface, was used.

3.3. Cell treatments

Cells were pretreated with 500 ng/mL LPS (Sigma Aldrich, *Escherichia coli* O111:B4) or 20 µg/mL polyinosinic:polycytidylic acid (poly(I:C), high molecular weight, Invivogen) for 24 hours. Cells were also transfected with 20 µg poly(I:C) 24 h prior to the experiment using Lipofectamine 3000 transfection reagent (Invitrogen) according to manufacturer's instructions. For transfection of one well (volume is 500 µL), 1 µL of poly(I:C) was mixed with 0,75 µL of LIPO-3000 reagents, 1 µL of P3000 reagents, and 50 µL of OPTI-MEM medium. The mix was vortexed, incubated for 15 min at room temperature, and then added to the cells.

3.4. Phagocytosis assay

To get the cell debris for phagocytosis experiment, N2A cells were treated for 24 h with 2 µM staurosporine (STS, Santa Cruz), an apoptosis-inducing bacterial toxin. After the treatment, the debris was collected in a 50 mL Falcon tube and centrifuged (1500 rpm, 5 min). Supernatant was thrown away, and the pelleted debris was frozen at -80°C until the experiments. For the experiments, N2A debris was stained with 10 µM carboxyfluorescein succinimidyl ester (CFSE, eBioscience), a cell-permeable fluorescent dye that binds covalently to proteins. The amount of debris that was used was 3x the number of cells per well, so ~300 000 cells/ well. N2A debris was washed 2x with PBS (1500 rpm, 5 min) and resuspended in 500 µL of PBS. CFSE was added to the final concentration of 10 µM, followed by incubation in the dark (20 min, room temperature). 5 ml of complete RPMI was added and the debris

was incubated for 5 min on ice. The debris was washed two more times with complete medium and resuspended in complete BMDM medium. N2A cell debris (dN2A) stained with CFSE was added to the cells (100 μ L/well). The plate was then centrifuged (5 min, 1000 rpm) to spin down dN2A onto the cells. The N2A debris was co-cultured with cells for 5 h. Besides the LPS and the poly(I:C) treatments 24 h before adding dN2A, cells were also treated with 2 μ M Cytochalasin D (CytoD, Sigma Aldrich) 30 min before, and 200 nM Bafilomycin A1 (BafA1, Sigma Aldrich) was added 4 h before samples were collected. CytoD, an actin inhibitor that effectively blocks phagocytosis, was used as control to ensure the CFSE signal detected in BMDMs comes from phagocytosed N2A debris, and not fragments stuck to the cell surface. BafA1, an inhibitor of late stage phagosome-lysosome fusion, was used to prevent N2A debris degradation once phagocytosed, and increase CFSE signal. LPS and poly(I:C) were used to trigger inflammation in order to examine how inflammatory environment affects phagocytosis. After 5 h, cells were collected for analysis via flow cytometry.

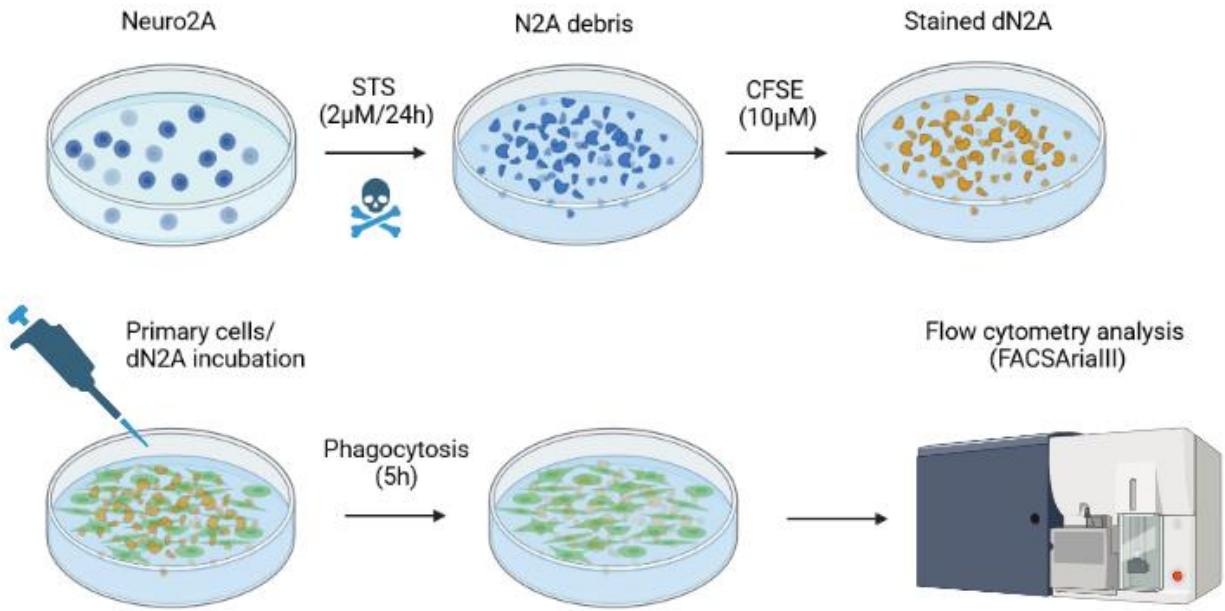


Figure 4 Phagocytosis experiment outline. Neuro2A cells were treated with 2 μM STS for 24 h and stained with 10 μM CFSE. The stained debris was then dripped on the primary cells and incubated for 5h. The phagocytosis of the debris by the primary cells was analyzed and assessed with flow cytometry.

3.5. Flow cytometry

BMDM/Microglia and dN2A co-cultures were lifted from the plate using EDTA following the same protocol as described earlier and moved into 2 mL safe-lock tubes. Samples were resuspended in 200 μ L of FACS flow medium (PBS with 2% FBS and 0,05% sodium azide (Carl Roth)) and washed two times with FACS flow (5 min, 1500 rpm). Dead cells were labeled with 4',6-diamidino-2-phenylindole (DAPI, Sigma Aldrich), a blue-fluorescent DNA-intercalating dye that penetrates into the nuclei of dead cells. The cells were incubated with 300 nM DAPI for 5 min in the dark at room temperature. After incubation with DAPI, cells were centrifuged once with 1 mL of FACS flow (5 min, 1500 rpm). Cells were then resuspended in 200 μ L of FACS flow and filtered through 35 μ m strainers into polystyrene round-bottom FACS tubes containing another 200 μ L of FACS flow.

Flow cytometry was performed on BD FACSAria III (BD Biosciences). Compensation tubes comprised unstained cells and the following single-color samples: DAPI-stained cells, PKH26-stained cells, and CFSE-stained dN2A. Samples were gated on forward and side scatter (FSC, SSC) to identify cells and separate them from the debris. Gating DAPI⁻ events on DAPI/FSC dot plot was done to identify viable/live cells. BMDMs were identified as PKH26⁺ on the PKH26/FSC dot plot from the subset of live cells. PKH26⁺/CFSE⁺ events were identified as BMDMs that phagocytosed N2A debris. The results were analyzed in FlowJo software (Tri Star).

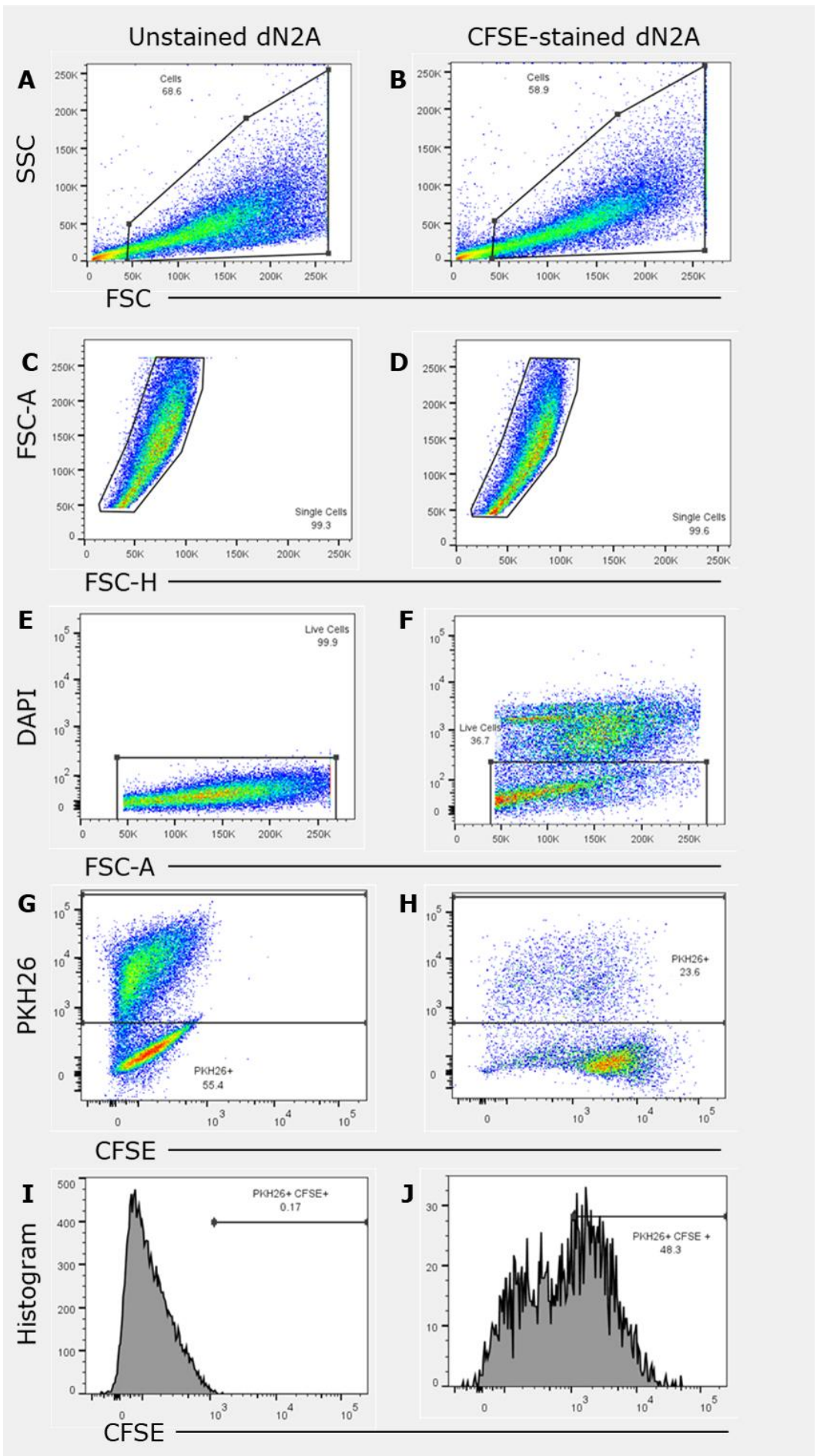


Figure 5 FlowJo analysis outline. Gating for all the subsequent samples was done on WT PKH26-stained cells treated with unstained dN2A. PKH26-stained WT cells treated with CFSE-stained dN2A are shown in the right column for comparison. The first step was to separate the cells from debris. On the FSC/SSC plot gating was done to exclude the smallest events (debris) (A,B). The next step was to determine which events were singlets (1 event = 1 cell). On the FSC-H/FSC-A plot, gating was done to exclude the events which departed from the main event cluster (C,D). Then live cells were gated, on the FSC-A/DAPI plot live cells were those that did not have a DAPI signal (E,F). The next step was gating the PKH26-stained macrophages on the CFSE/PKH26 plot (G,H). The final step was gating the CFSE/histogram plot so that there was no CFSE signal in the WT cells treated with unstained debris (I). In the subsequent samples, which were treated with CFSE-stained debris, there was CFSE signal (J), and the amount and intensity of the signal was used in statistical analysis.

3.6. Statistical analysis

The results were analyzed in GraphPad Prism software. Data shown represents means of at least three independent experiments. Student's t-test was used to determine statistical significance. A p value lesser than 0,05 was considered as statistically significant.

4. Results

4.1. Frozen N2A debris does not affect phagocytosis in WT and OPTN^{470T} BMDMs

In order to simplify the phagocytosis assay, we compared whether apoptotic N2A debris being frozen instead of dyed and used immediately after the 24 h STS treatment had an effect on phagocytosis level. We compared basal level of phagocytosis after 5 h of incubating WT and OPTN^{470T} BMDMs with frozen and “fresh” N2A debris, as well as frozen debris from primary neurons. All debris was stained with CFSE on the day of the experiment. BMDMs were stained with PKH26 dye and analyzed by flow cytometry. Phagocytosing BMDMs were identified as live (DAPI⁻) PKH⁺ CFSE⁺ events on the dot plot diagram, and CFSE signal threshold was determined using unstained dN2A (Figure 7A). Two parameters were used to measure the efficacy of phagocytosis: the frequency of DAPI⁻ PKH⁺ CFSE⁺ BMDMs and mean fluorescence intensity (MFI) of CFSE in those cells. The frequency gives us information about the number of BMDMs that have phagocytosed the debris, and the MFI represents phagocytic ability of the cells. When it comes to the number of phagocytosing cells, frozen primary neuron debris and “fresh” N2A debris had similar results, around 50%. Frozen N2A debris was phagocytosed by a larger number of the cells, closer to 80% (Figure 7B). When the MFI values were normalized to WT “fresh” N2A debris, OPTN^{470T} BMDMs phagocytosed it 25% compared to WT. Frozen N2A debris was again phagocytosed more, 74% more by the WT BMDMs and 44% more by the OPTN^{470T} BMDMs. Frozen primary neurons had a similar result to “fresh” N2A debris, WT BMDMs phagocytosed 15% more compared to the baseline, and OPTN^{470T} BMDMs phagocytosed 11% less (Figure 7C). It is important to note that the preliminary experiment has been performed only once, and that the results of using the frozen N2A debris could have been affected by the amount of debris being put on the cells. Nevertheless, the results indicated that using

frozen N2A debris, as well as frozen debris from primary neurons did not negatively impact the experiment outcome, hence why in the following experiments frozen N2A debris was used.

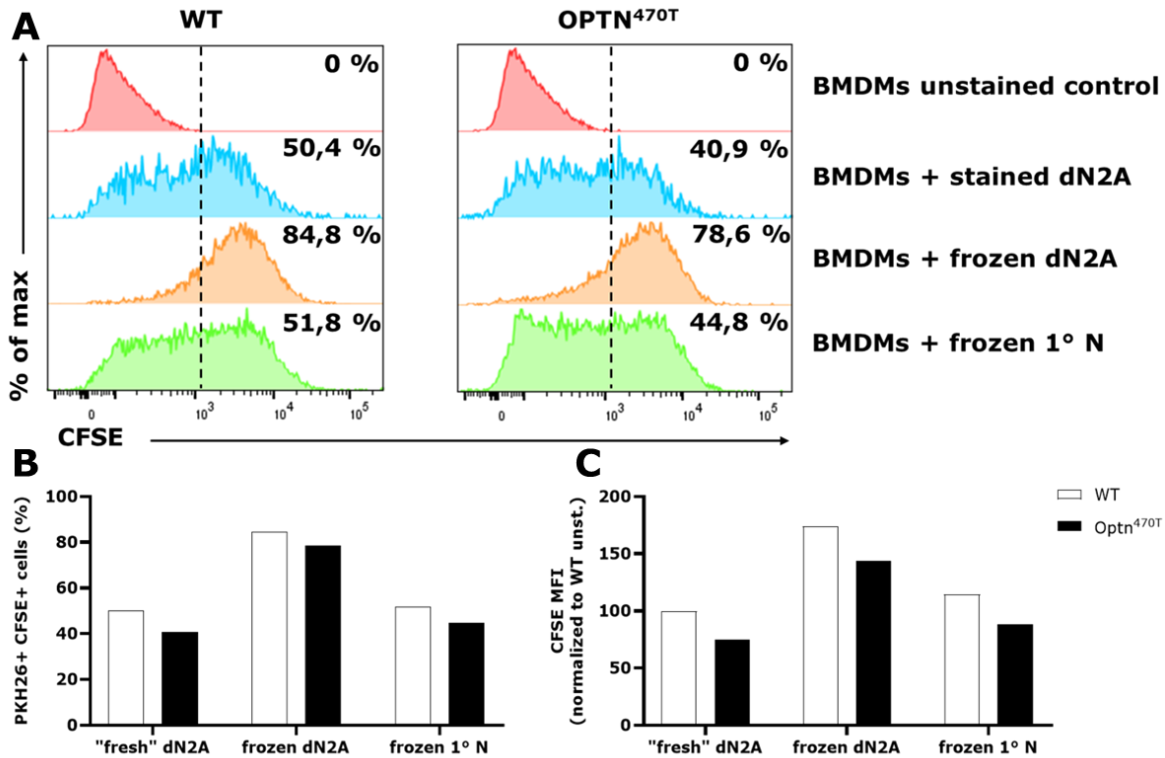


Figure 6 The efficiency of phagocytosis is equal when frozen N2A debris is used. WT and OPTN^{470T} PKH26-stained BMDMs from mice aged 2 years were incubated with CFSE-stained dN2A for 5 h. The dN2A was either previously treated with STS for 24 h and frozen at -80°C or treated with STS 24h prior and used "fresh". In both cases, the dN2A was stained with CFSE on the day of the experiment. Upon harvesting BMDMs were analyzed using flow cytometry. (A) Flow cytometry histograms show frequency of dN2A phagocytosis as percentage of PKH26+ CFSE+ BMDMs (gated in the population of live BMDMs). (B) Bar graph showing percentage of PKH26+ CFSE+ BMDMs. (C) Bar graph showing CFSE MFI of PKH26+ CFSE+ BMDMs. The MFI values were normalized to WT untreated BMDMs. Data was analyzed using FlowJo and GraphPad. There was no statistical analysis done since this initial experiment was performed once.

4.2. Optineurin insufficiency does not diminish phagocytosis of N2A debris in BMDMs from young mice

After optimizing the phagocytosis assay, we compared phagocytic ability of WT and OPTN^{470T} BMDMs generated from young mice. For the experiment, PKH26-stained BMDMs were incubated with CFSE-stained N2A debris for 5 hours. Untreated WT cells from percentage of phagocytic cells of 60% (Fig. 7A). To ensure the CFSE signal detected in BMDMs comes from phagocytosed N2A debris, we used CytoD, an actin inhibitor that effectively blocks phagocytosis. CytoD treatment 30 min before adding the debris lowered the amount of phagocytic cells by more than half. This indicated that the signal comes from the dN2A phagosomes. OPTN^{470T} cells had the same percentage of phagocytic cells as WT cells, and CytoD lowered that amount by half, as well. Inflammatory environment achieved through LPS treatment 24 h prior to adding the debris did not significantly change the amount of phagocytic cells in WT and OPTN^{470T} BMDMs. To test if blockade of lysosomal degradation would uncover the difference in phagocytosis of WT and OPTN^{470T} BMDMs, we precluded lysosomal degradation by blocking their acidification with BafA1 1 h after adding the debris. As expected, the number of phagocytic cells did not change. Combined treatment with LPS and BafA1 slightly increased phagocytosis in WT BMDMs, but not significantly, and in OPTN^{470T} cells there was no difference. Once MFI was normalized, there was no difference between the phagocytic ability of untreated WT and OPTN^{470T} cells (Fig. 7B). CytoD treatment lowered the phagocytic ability by half in WT cells, and more than that in OPTN^{470T} cells. LPS treatment did not lead to an increase in CFSE signal in WT and OPTN^{470T} cells. However, BafA1 treatment led to an increase in CFSE signal; it doubled in WT cells, and almost doubled in OPTN^{470T} cells. This indicates that there was a certain amount of phagocytosed debris being degraded through autophagy or lysosomes. The combined treatment of LPS and BafA1 did not have a cumulative effect on the cells, indicating that

inflammatory environment does not influence the rate of lysosomal degradation. These results indicate that phagocytosed N2A debris was being degraded in late phagosomes or lysosomes, and BafA1 successfully blocked lysosomal degradation. Optineurin deficiency had no role in the phagocytosis of dN2A debris by WT and OPTN^{470T} BMDMs from young mice.

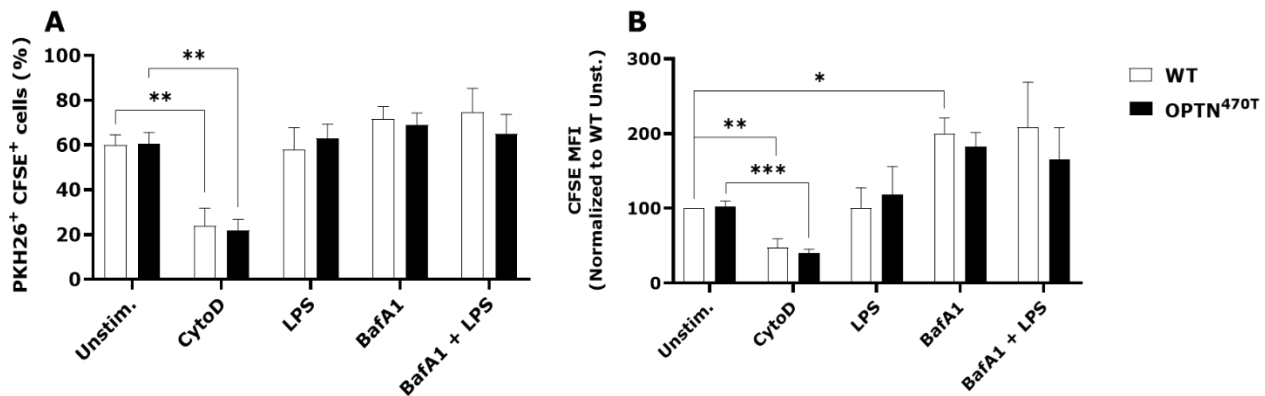


Figure 7 Optineurin does not play a role in phagocytosis of dN2A in murine BMDMs from young mice. WT and OPTN^{470T} PKH26-stained BMDMs from mice aged 3 months were incubated with CFSE-stained dN2A for 5 h. BMDMs were treated with CytoD, LPS, poly(I:C), or left untreated. Upon harvesting BMDMs were analyzed using flow cytometry. (Left) Bar graph showing percentage of PKH26⁺ CFSE⁺ BMDMs. (Right) Bar graph showing CFSE MFI of PKH26⁺ CFSE⁺ BMDMs. The MFI values were normalized to WT untreated BMDMs. Data was analyzed using FlowJo and GraphPad. Data are shown as mean ± SEM from BMDMs from 5 experiments. (unpaired t-test; *p<0,05, **p<0,01, ***p<0,001)

4.3. Optineurin insufficiency does not diminish phagocytosis of N2A debris in BMDMs from aged mice

After seeing that optineurin insufficiency had no effect in cells from young mice, we theorized that perhaps certain age-related immune dysfunctions might also be a factor. To test that hypothesis, we compared phagocytic ability of WT versus OPTN^{470T} BMDMs from mice aged 2 years. WT and OPTN^{470T} cells were incubated with CFSE-stained N2A debris for 5 h. In untreated BMDMs mean level of phagocytosis was around 35% in WT BMDMs (Figure 8A). When treated with CytoD, the WT cells showed minimal CFSE signal. A very similar effect was also seen in OPTN^{470T} cells, both untreated and treated with CytoD. LPS slightly increased phagocytosis in WT and OPTN^{470T} cells. As another inflammatory stimulant we used poly(I:C), a synthetic analog of viral DNA that

binds to different receptors than LPS and activates different signaling pathways. Treatment with transfected poly(I:C) slightly improved phagocytosis, more so in WT than OPTN^{470T} cells. When poly(I:C) was added externally, the effect was lesser in both genotypes. Neither BafA1 treatment or BafA1 combined with LPS significantly changed number of phagocytic cells in either genotype. Once normalized to WT untreated cells, CFSE MFI were nearly identical in untreated WT and OPTN^{470T} cells (Figure 8B). CytoD treatment lowered the CFSE MFI values by half. Treatment with LPS lead to CFSE MFI growing significantly in WT cells, but not OPTN^{470T} cells. Poly(I:C) treatment led to a slight increase in the phagocytic ability of BMDMs, more so when transfected, but it was not significant. BafA1 treatment led to a higher CFSE signal, which was not significant due to variation, but it was significant in both genotypes when combined with LPS treatment. Taken together, the results indicate that optineurin insufficiency did not have an effect on phagocytosis of neuronal debris by BMDMs from aged mice. Phagocytic ability of WT cells grew significantly when LPS was added, but not with poly(I:C) treatments. The difference was not significant in OPTN^{470T} cells.

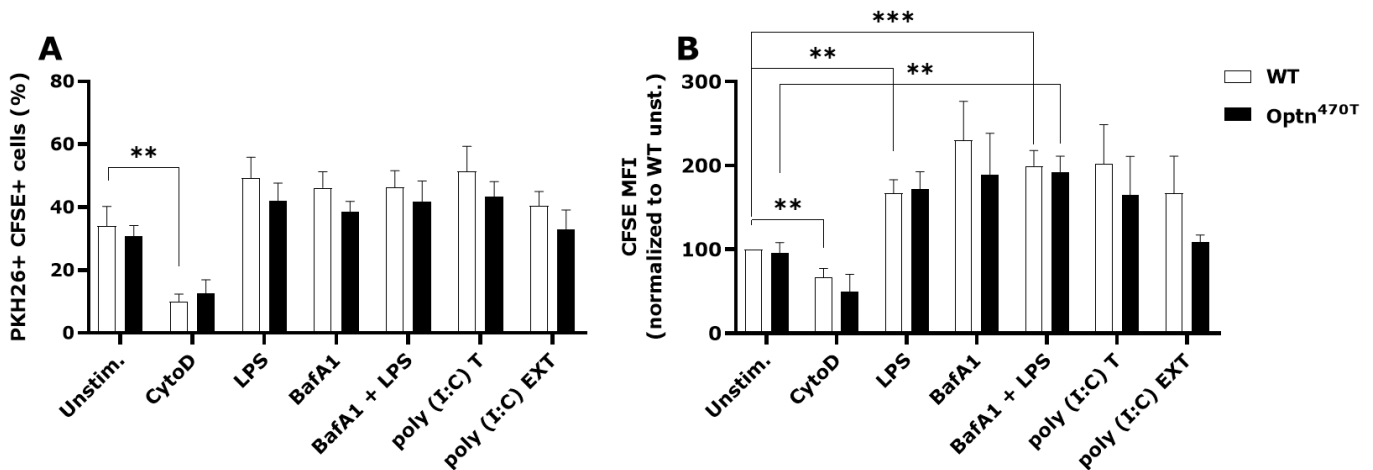


Figure 8 Optineurin does not play a role in phagocytosis of dN2A in murine BMDMs from aged mice. WT and OPTN^{470T} PKH26-stained BMDMs from mice aged 2 years were incubated with CFSE-stained dN2A for 5 h. BMDMs were treated with CytoD, LPS, BafA1, a combination of LPS and BafA1, poly(I:C), or left untreated. Upon harvesting BMDMs were analyzed using flow cytometry. (A) Bar graph showing percentage of PKH26+ CFSE+ BMDMs. (B) Bar graph showing CFSE MFI of PKH26+ CFSE+ BMDMs. The MFI values were normalized to WT untreated BMDMs. Data was analyzed using FlowJo and GraphPad. Data are shown as mean ± SEM from BMDMs from 6 experiments (from 6 individual mice). (unpaired t-test; **p<0,01, ***p<0,001)

4.4. Phagocytosis in WT and OPTN^{470T} BMDMs becomes impaired with age

Once the phagocytosis assay was done on BMDMs from both younger and older mice, we compared their percentages of phagocytic cells. In WT BMDMs the level of phagocytosis was statistically lower in untreated cells (Figure 9A). There was no difference after CytoD treatment in the level of phagocytosis of WT cells. The difference was also not statistically different when cells were treated with LPS. The level of phagocytosis of WT cells from older mice after BafA1 treatment was significantly lower, as it was after the combined treatment of LPS and BafA1. The difference between untreated OPTN^{470T} cells from young and old mice was even bigger than in WT cells (Figure 9B). As in the WT cells, there was no difference in the level of phagocytosis after CytoD and LPS treatment in OPTN^{470T} cells. There was a difference in OPTN^{470T} cells from young and old mice treated with BafA1, as well as in those treated with BafA1 and LPS. These results indicate that phagocytosis becomes impaired with age, but cells from both young and old mice respond equally to inflammatory environment.

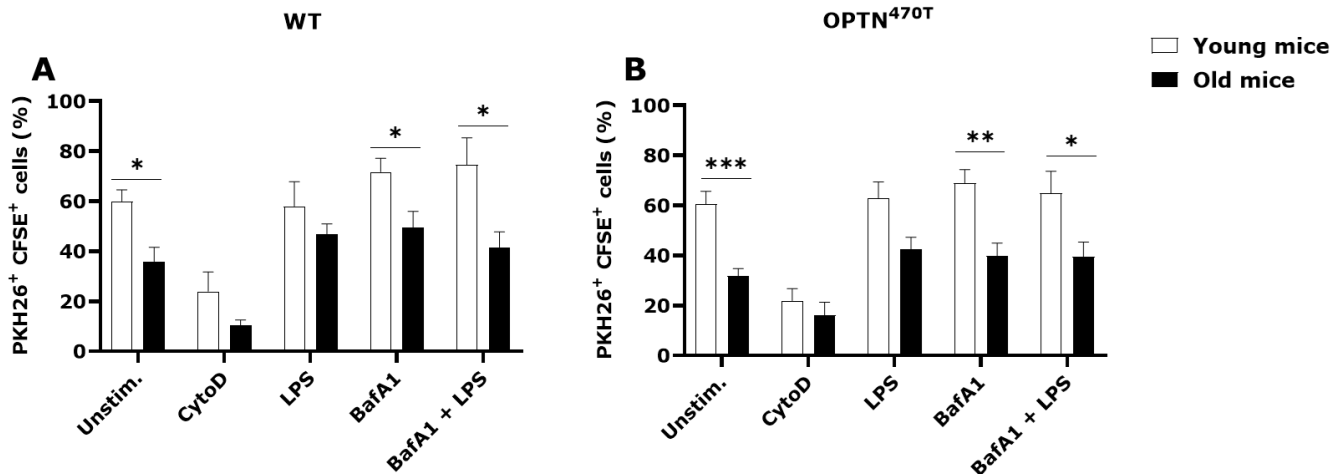


Figure 9 Phagocytosis in WT and OPTN^{470T} BMDMs becomes impaired with age. WT and OPTN^{470T} PKH26-stained BMDMs from mice aged 2 years and 3 months were incubated with CFSE-stained dN2A for 5 h. BMDMs were treated with CytoD, LPS, BafA1, a combination of LPS and BafA1, or left untreated. (A) Bar graph showing the percentage of PKH26+ CFSE+ WT BMDMs. (B) Bar graph showing the percentage of PKH26+ CFSE+ KI BMDMs. Data was analyzed using FlowJo and GraphPad. Data are shown as mean \pm SEM from 5 experiments done on BMDMs from young mice and 6 experiments done on BMDMs from old mice. (unpaired t-test; * p <0.05, ** p <0.01, *** p <0.001)

4.5. Optineurin insufficiency does not diminish phagocytosis of neuronal debris in WT and OPTN^{470T} microglia

Since microglia have been shown to be active in presymptomatic stages of ALS, we also did the phagocytosis assay was also done on primary murine microglia. Microglia were stained with Far Red and incubated with CFSE-stained dN2A for 5 h. In untreated cells there was no difference in the level of phagocytosis between the genotypes, though the level was higher than in primary BMDMs, around 80%. CytoD lowered the level of phagocytosis numbers to 38% in WT microglia and 49% in OPTN^{470T} microglia. BafA1 and LPS treatments did significantly affect the percentage of WT and OPTN^{470T} phagocytic cells. Once the CFSE was normalized to WT untreated cells, there was no difference between the WT and OPTN^{470T} microglia. There was also no difference in CFSE MFI after the CytoD treatment. BafA1 treatment increased the CFSE signal by more than double in WT and OPTN^{470T} cells, demonstrating that in microglia there is also a significant amount of phagocytosed debris that

gets degraded via autophagy over the course of the experiment. LPS treatment also increased the CFSE MFI, but to a lesser degree. Overall, LPS and BafA1 treatments affected the CFSE MFI signal, but as in BMDMs, optineurin did not influence phagocytosis of dN2A by primary murine microglia.

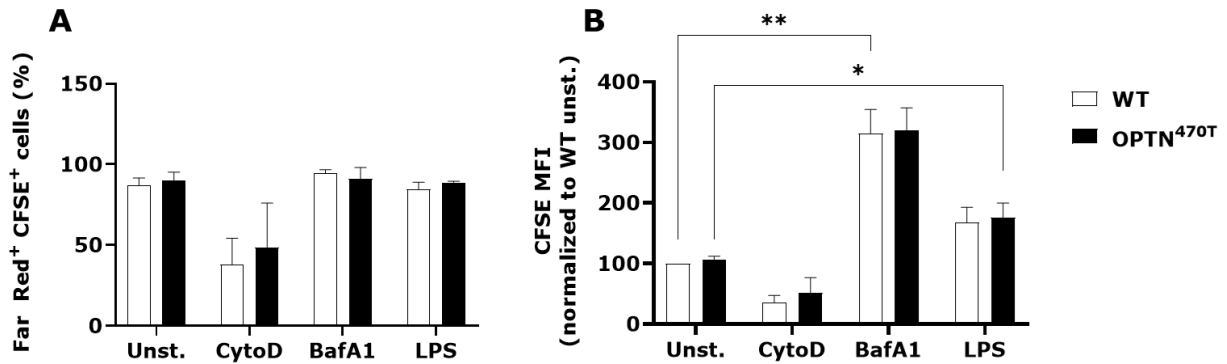


Figure 10 Optineurin does not influence phagocytosis of dN2A in WT and OPTN^{470T} microglia. WT and OPTN^{470T} Far Red-stained murine microglia were incubated with CFSE-stained dN2A for 5 h. BMDMs were treated with CytoD, LPS, BafA1, or left untreated. (A) Bar graph showing the percentage of PKH26+ CFSE+ WT BMDMs. (B) Bar graph showing the percentage of PKH26+ CFSE+ KI BMDMs. Data was analyzed using FlowJo and GraphPad. Data are shown as mean \pm SEM. (unpaired t-test; *p<0.05, **p<0.01) n=3

5. Discussion

The role of microglia, as resident macrophages in the CNS, is clearing out cellular debris to prevent immune activation in the CNS. The role of microglial phagocytosis in neurodegenerative disorders is not yet clear. It has been found that hSOD1 transgenic rats have active phagocytic microglia in their spinal cord during the presymptomatic stage of the disease, before any neuronal loss is detected (37). A recent study done on microglia-like cells from sALS patients has shown that those cells have impaired phagocytic ability that matched the progression of the disease (38). Important to note that was not specified if any of the patients in that study had an *OPTN* mutation. The research from our lab on *OPTN* KO BV2 microglial cell lines showed slightly impaired phagocytosis compared to the WT (39), but there has not been any research done on the efficacy of phagocytosis in primary cells generated from *OPTN*^{470T} *OPTN*-insufficient mouse model. In our research we used BDMs and microglia generated from WT and *OPTN*^{470T} mice, and modified a phagocytosis assay previously used in our lab to analyze phagocytosis of BV2 cell lines (39). There was no difference between the genotypes in any of the primary cells used in number of phagocytic cells or their phagocytic ability when cells were left untreated. These results suggested that at a basal state optineurin insufficiency does not diminish phagocytosis. Previous research done on BV2 cell lines has shown slightly impaired phagocytosis in *OPTN* KO cells. One possible reason for that is off-target binding of siRNA that was used to get KO BV2 cells, which could have affected other signaling pathways, and indirectly affected phagocytosis. Another possible reason might be the fact that BV2 cells suffered from complete optineurin deficiency, while the *OPTN*^{470T} cells represent a model of optineurin insufficiency, only lacking the ubiquitin-binding domain. In the future it would be useful to repeat the experiment on other optineurin insufficiency or deficiency models, maybe even those that are missing a region of the protein other than the ubiquitin-binding one, to

elucidate if there is a certain region of optineurin that has interactions which could affect phagocytosis.

BafA1 treatment affected the CFSE signal, suggesting that at least some of the phagocytosed debris was being degraded over the course of the experiment in phagosomes and/or lysosomes. Since type I IFNs have been shown to have a role in induction of autophagy (42), levels of IFN- β present in the cells would be of great interest.

It is important to note that BafA1 and CytoD treatments did not lead to an expected outcome regarding the number of phagocytic cells and the CFSE signal in every experiment with BMDMs from older mice. Whether the reason for that is the freeze thaw process (BafA1 and CytoD are kept at -20°C), human error, or some innate trait of the cells due to age of the mice, it remains to be seen through future experiments, and perhaps change the storage conditions of BafA1 and CytoD.

When compared to BMDMs from younger mice, BMDMs from mice aged 2 years showed a lower percentage of phagocytic cells. A possible reason for the differences between the cells from young and old mice could have been different staining of the debris, or a different amount of the debris dripped onto the cells. An experiment was done parallel with cells from both young and old WT and OPTN^{470T} mice, using the same "batch" of CFSE-stained debris (data not shown), and the procedure of adding debris onto the cells was done by the same person. The results confirmed that there was indeed a difference, and the factor of human error or discrepancies in debris staining and the experiment itself was removed as a possible cause of the differences.

The only condition besides CytoD without significant difference between the cells from young and old mice was the LPS treatment. This is interesting because one would expect that the cells from older mice would not be as reactive to stimuli, since studies have shown that aged microglia are not as responsive to stimuli (34). A study has shown that LPS actually impairs the

phagocytosis of macrophages (43). This study observed the rate of phagocytosis for 24 h after adding LPS to macrophages. It is quite possible that rate of phagocytosis in our experiment would be higher after LPS was just added; one way to test that would be different time points for LPS treatment as conditions in the experiment.

Since BMDMs were not treated with poly(I:C), we did not have the data necessary to compare the rate of phagocytosis between the BMDMs generated from younger and older mice. The phagocytosis experiment should be repeated on BMDMs generated from young mice pre-treated with poly(I:C). Depending on those results, it might imply a certain signaling pathway with the process of phagocytosis and open up new venues of research.

6. Conclusion

In order to study the potential optineurin has in the process of phagocytosis, we performed a flow cytometry based phagocytosis assay on WT and OPTN^{470T} primary BMDMs and microglia. The rate of phagocytosis stayed the same between the genotypes throughout the experiment. BafA1 treatment affected the CFSE signal, suggesting that at least a part of the phagocytosed debris in phagosomes was being removed via autophagy and/or lysosomes. The phagocytosis assay was also done on BMDMs from mice aged 2 years, and there was a difference in the number of phagocytic cells when compared to BMDMs from younger mice, suggesting that phagocytosis becomes less efficient with age. To further study the possible effect of optineurin during phagocytosis, cytokine levels should be analyzed after the phagocytosis experiment, and compared. These results suggest that optineurin insufficiency does not diminish phagocytosis, but the phagocytosis assay itself opens up possibilities in researching the potential role of this cellular process in ALS.

7. Literature

1. Toth RP, Atkin JD. Dysfunction of Optineurin in Amyotrophic Lateral Sclerosis and Glaucoma. *Front Immunol.* 2018;9:1017.
2. Minegishi Y, Nakayama M, Iejima D, Kawase K, Iwata T. Significance of optineurin mutations in glaucoma and other diseases. *Prog Retin Eye Res.* 2016 Nov;55:149–81.
3. Marin B, Boumédiène F, Logroscino G, Couratier P, Babron MC, Leutenegger AL, et al. Variation in worldwide incidence of amyotrophic lateral sclerosis: a meta-analysis. *Int J Epidemiol.* 2017 Feb 1;46(1):57–74.
4. Brown RH, Al-Chalabi A. Amyotrophic Lateral Sclerosis. *N Engl J Med.* 2017 Jul 13;377(2):162–72.
5. State of play in amyotrophic lateral sclerosis genetics - PubMed [Internet]. [cited 2022 Jul 12]. Available from: <https://pubmed.ncbi.nlm.nih.gov/24369373/>
6. Chia R, Chiò A, Traynor BJ. Novel genes associated with amyotrophic lateral sclerosis: diagnostic and clinical implications. *Lancet Neurol.* 2018 Jan;17(1):94–102.
7. (4) (PDF) Optineurin Dysfunction in Amyotrophic Lateral Sclerosis: Why So Puzzling? [Internet]. [cited 2022 Jul 23]. Available from: https://www.researchgate.net/publication/350586574_Optineurin_Dysfunction_in_Amyotrophic_Lateral_Sclerosis_Why_So_Puzzling
8. Bendotti C, Marino M, Cheroni C, Fontana E, Crippa V, Poletti A, et al. Dysfunction of constitutive and inducible ubiquitin-proteasome system in amyotrophic lateral sclerosis: Implication for protein aggregation and immune response. *PROG NEUROBIOL.* 2012 May;97(2):101–26.
9. Optineurin Deficiency and Insufficiency Lead to Higher Microglial TDP-43 Protein Levels - PubMed [Internet]. [cited 2022 Jul 23]. Available from: <https://pubmed.ncbi.nlm.nih.gov/35743272/>
10. Markovinovic A, Cimbro R, Ljutic T, Kriz J, Rogelj B, Munitic I. Optineurin in amyotrophic lateral sclerosis: Multifunctional adaptor protein at the crossroads of different neuroprotective mechanisms. *Prog Neurobiol.* 2017 Jul;154:1–20.
11. Slowicka K, Vereecke L, van Loo G. Cellular Functions of Optineurin in Health and Disease. *Trends Immunol.* 2016 Sep;37(9):621–33.
12. TBK1: a new player in ALS linking autophagy and neuroinflammation - PubMed [Internet]. [cited 2022 Jul 18]. Available from: <https://pubmed.ncbi.nlm.nih.gov/28148298/>
13. Rezaie T, Child A, Hitchings R, Brice G, Miller L, Coca-Prados M, et al. Adult-onset primary open-angle glaucoma caused by mutations in optineurin. *Science.* 2002 Feb 8;295(5557):1077–9.
14. Gleason CE, Ordureau A, Gourlay R, Arthur JSC, Cohen P. Polyubiquitin Binding to Optineurin Is Required for Optimal Activation of TANK-

- binding Kinase 1 and Production of Interferon β . *J Biol Chem*. 2011 Oct 14;286(41):35663–74.
15. Munitic I, Giardino Torchia ML, Meena NP, Zhu G, Li CC, Ashwell JD. Optineurin insufficiency impairs IRF3 but not NF- κ B activation in immune cells. *J Immunol*. 2013 Dec 15;191(12):6231–40.
 16. Meena NP, Zhu G, Mittelstadt PR, Giardino Torchia ML, Pourcelot M, Arnoult D, et al. The TBK1-binding domain of optineurin promotes type I interferon responses. *FEBS Lett*. 2016;590(10):1498–508.
 17. Slowicka K, Vereecke L, Mc Guire C, Sze M, Maelfait J, Kolpe A, et al. Optineurin deficiency in mice is associated with increased sensitivity to *Salmonella* but does not affect proinflammatory NF- κ B signaling. *European Journal of Immunology*. 2016;46(4):971–80.
 18. Nakazawa S, Oikawa D, Ishii R, Ayaki T, Takahashi H, Takeda H, et al. Linear ubiquitination is involved in the pathogenesis of optineurin-associated amyotrophic lateral sclerosis. *Nat Commun*. 2016 Aug 24;7:12547.
 19. Liu Z#, Li H#, Hong C, Yue T, Chen C, Wang Z, et al. ALS-Associated E478G Mutation in Human OPTN (Optineurin) Promotes Inflammation and Induces Neuronal Cell Death. *Front Immunol* [Internet]. 2018 [cited 2020 Nov 19];9. Available from: <https://www.frontiersin.org/articles/10.3389/fimmu.2018.02647/full>
 20. Akizuki M, Yamashita H, Uemura K, Maruyama H, Kawakami H, Ito H, et al. Optineurin suppression causes neuronal cell death via NF- κ B pathway. *J Neurochem*. 2013 Sep;126(6):699–704.
 21. Béland LC, Markovinovic A, Jakovac H, De Marchi F, Bilic E, Mazzini L, et al. Immunity in amyotrophic lateral sclerosis: blurred lines between excessive inflammation and inefficient immune responses. *Brain Commun*. 2020 Aug 13;2(2):fcaa124.
 22. Lino MM, Schneider C, Caroni P. Accumulation of SOD1 mutants in postnatal motoneurons does not cause motoneuron pathology or motoneuron disease. *J Neurosci*. 2002 Jun 15;22(12):4825–32.
 23. Clement AM, Nguyen MD, Roberts EA, Garcia ML, Boillée S, Rule M, et al. Wild-type nonneuronal cells extend survival of SOD1 mutant motor neurons in ALS mice. *Science*. 2003 Oct 3;302(5642):113–7.
 24. Boillée S, Yamanaka K, Lobsiger CS, Copeland NG, Jenkins NA, Kassiotis G, et al. Onset and progression in inherited ALS determined by motor neurons and microglia. *Science*. 2006 Jun 2;312(5778):1389–92.
 25. Yamanaka K, Chun SJ, Boillee S, Fujimori-Tonou N, Yamashita H, Gutmann DH, et al. Astrocytes as determinants of disease progression in inherited amyotrophic lateral sclerosis. *Nat Neurosci*. 2008 Mar;11(3):251–3.

26. Zhao W, Beers DR, Bell S, Wang J, Wen S, Baloh RH, et al. TDP-43 activates microglia through NF- κ B and NLRP3 inflammasome. *Exp Neurol*. 2015 Nov;273:24–35.
27. Geloso MC, Corvino V, Marchese E, Serrano A, Michetti F, D’Ambrosi N. The Dual Role of Microglia in ALS: Mechanisms and Therapeutic Approaches. *Frontiers in Aging Neuroscience* [Internet]. 2017 [cited 2022 Jul 25];9. Available from: <https://www.frontiersin.org/articles/10.3389/fnagi.2017.00242>
28. Philips T, Robberecht W. Neuroinflammation in amyotrophic lateral sclerosis: role of glial activation in motor neuron disease. *Lancet Neurol*. 2011 Mar;10(3):253–63.
29. Gravel M, Béland LC, Soucy G, Abdelhamid E, Rahimian R, Gravel C, et al. IL-10 Controls Early Microglial Phenotypes and Disease Onset in ALS Caused by Misfolded Superoxide Dismutase 1. *J Neurosci*. 2016 Jan 20;36(3):1031–48.
30. Beers DR, Zhao W, Liao B, Kano O, Wang J, Huang A, et al. Neuroinflammation modulates distinct regional and temporal clinical responses in ALS mice. *Brain Behav Immun*. 2011 Jul;25(5):1025–35.
31. Liao B, Zhao W, Beers DR, Henkel JS, Appel SH. Transformation from a neuroprotective to a neurotoxic microglial phenotype in a mouse model of ALS. *Exp Neurol*. 2012 Sep;237(1):147–52.
32. Satyam SM, Bairy LK. Neuronutraceuticals Combating Neuroinflammation: Molecular Insights and Translational Challenges—A Systematic Review. *Nutrients*. 2022 Jul 23;14(15):3029.
33. Innate immune receptor expression in normal brain aging - PubMed [Internet]. [cited 2022 Aug 10]. Available from: <https://pubmed.ncbi.nlm.nih.gov/17293054/>
34. Streit WJ, Miller KR, Lopes KO, Njie E. Microglial degeneration in the aging brain--bad news for neurons? *Front Biosci*. 2008 May 1;13:3423–38.
35. Uribe-Querol E, Rosales C. Phagocytosis: Our Current Understanding of a Universal Biological Process. *Frontiers in Immunology* [Internet]. 2020 [cited 2022 Sep 3];11. Available from: <https://www.frontiersin.org/articles/10.3389/fimmu.2020.01066>
36. Yu F, Wang Y, Stetler AR, Leak RK, Hu X, Chen J. Phagocytic microglia and macrophages in brain injury and repair. *CNS Neurosci Ther*. 2022 Sep;28(9):1279–93.
37. Sanagi T, Yuasa S, Nakamura Y, Suzuki E, Aoki M, Warita H, et al. Appearance of phagocytic microglia adjacent to motoneurons in spinal cord tissue from a presymptomatic transgenic rat model of amyotrophic lateral sclerosis. *J Neurosci Res*. 2010 Sep;88(12):2736–46.
38. Quek H, Cuní-López C, Stewart R, Colletti T, Notaro A, Nguyen TH, et al. ALS monocyte-derived microglia-like cells reveal cytoplasmic TDP-

- 43 accumulation, DNA damage, and cell-specific impairment of phagocytosis associated with disease progression. *Journal of Neuroinflammation*. 2022 Feb 28;19(1):58.
39. Rob M. Karakterizacija uloge optineurina u regulaciji upalnih signala u mikroglijalnim i neuronalnim staničnim linijama [Internet] [info:eu-repo/semantics/masterThesis]. University of Rijeka. Department of Biotechnology; 2018 [cited 2022 Jul 12]. Available from: <https://urn.nsk.hr/urn:nbn:hr:193:162533>
40. Prtenjaca N, Rob M, Alam MS, Markovinovic A, Stuani C, Buratti E, et al. Optineurin Deficiency and Insufficiency Lead to Higher Microglial TDP-43 Protein Levels. undefined [Internet]. 2022 [cited 2022 Sep 13]; Available from: <https://www.semanticscholar.org/paper/Optineurin-Deficiency-and-Insufficiency-Lead-to-Prtenjaca-Rob/c9818dda85749aa8559aeb660409e360c3e63365>
41. Markovinović A. NEUROINFLAMMATION IN MICE WITH OPTINEURIN INSUFFICIENCY [Internet] [info:eu-repo/semantics/doctoralThesis]. University of Rijeka. Department of Biotechnology; 2019 [cited 2022 Sep 19]. Available from: <https://urn.nsk.hr/urn:nbn:hr:193:538797>
42. New function of type I IFN: induction of autophagy - PubMed [Internet]. [cited 2022 Sep 13]. Available from: <https://pubmed.ncbi.nlm.nih.gov/24428799/>
43. Feng X, Deng T, Zhang Y, Su S, Wei C, Han D. Lipopolysaccharide inhibits macrophage phagocytosis of apoptotic neutrophils by regulating the production of tumour necrosis factor α and growth arrest-specific gene 6. *Immunology*. 2011 Feb;132(2):287–95.